J|A|C|S
ARTICLES
Published on Web 02/13/2003

Carbon Dioxide-in-Water Microemulsions

C. Ted Lee, Jr.,[†] Won Ryoo,[†] P. Griffin Smith, Jr.,[†] Jose Arellano,[§] Daniel R. Mitchell,[‡] Richard J. Lagow,[‡] Stephen E. Webber,*[,‡] and Keith P. Johnston*[,†]

Contribution from the Department of Chemical Engineering and Department of Chemistry and Biochemistry, University of Texas at Austin, Austin, Texas 78712

Received January 28, 2002; E-mail: kpj@che.utexas.edu

Abstract: Liquid and supercritical carbon dioxide swell potassium carboxylate perfluoropolyether (PFPE-K) cylindrical micelles in water to produce novel CO_2-in-water (C/W) microemulsions. The swelling elongates the micelles significantly from 20 to 80 nm as the molar ratio of CO_2 in the micelles to surfactant (R_{CO2}) reaches approximately 8. As the micelles swell to form microemulsions, the solubility of pyrene increases by a factor of ca. 10. Fluorescence spectra suggest that pyrene resides primarily in the low-polarity micelle core rather than in the palisade region. The results illustrate the ability of C/W microemulsions to solubilize both lipophilic and fluorophilic substances simultaneously.

Introduction

Liquid or supercritical CO_2 ($T_c = 31$ °C, $P_c = 73.8$ bar) is nonpolar (unlike water, a highly structured fluid with strong intermolecular forces) with a low polarizability per volume and correspondingly weak van der Waals forces (unlike oils).[1] Consequently, CO_2 and water represent extremes of the solvent spectra. A unique property of supercritical fluids is the formation of solvent clusters, i.e., local solvent densities in excess of bulk densities near a solute, which augments solubilities.[2] Furthermore, the relatively large quadrupole moment of CO_2 enhances solubilities of certain polar hydrocarbons, e.g., benzoic acid and 2-naphthol,[3] in CO_2 relative to solvents such as ethane. As a result of these properties, dispersions of CO_2 in water are candidates for the solubilization of a wide range of fluorophilic, lipophilic, and hydrophilic materials.

Microscopic and macroscopic dispersions consisting of water-in-CO_2 (W/C) microemulsions and emulsions, respectively, have been formed recently.[4,5] These dispersions have been used to solubilize hydrophilic substances into CO_2 (e.g., salts,[6,7] water-soluble catalysts,[8] metal nanoparticles,[9−11] metal ions,[12] NMR[13] and electroactive[14] probes, proteins,[4,15] and enzymes[16,17]), to perform biphasic, metal-catalyzed, and enzyme-catalyzed reactions in CO_2, and to form porous polymers.[18] The formation of CO_2-continuous dispersions requires surfactants that are CO_2-soluble,[19] that preferentially curve about water in the case of microemulsions, and that have surfactant tails that are sufficiently solvated by CO_2 to minimize droplet interactions.[5,20] Most studies have used di-chained[21,22] or flexible fluorocarbon surfactants,[4,23,24] which have favorable CO_2−fluorocarbon compared to CO_2−hydrocarbon interactions.[25] Recently, micelles[26]

[†] Department of Chemical Engineering.
[‡] Department of Chemistry and Biochemistry.
[§] Current address: Department of Chemistry, University of Wisconsin, Madison, WI.

(1) O'Shea, K.; Kirmse, K.; Fox, M. A.; Johnston, K. P. *J. Phys. Chem.* **1991**, *95*, 7863.
(2) Eckert, C. A.; Knutson, B. L.; Debenedetti, P. G. *Nature (London)* **1996**, *383*, 313−318.
(3) Schmitt, W. J.; Reid, R. C. *J. Chem. Eng. Data* **1986**, *31*, 204−212.
(4) Johnston, K. P.; Harrison, K. L.; Clarke, M. J.; Howdle, S. M.; Heitz, M. P.; Bright, F. V.; Carlier, C.; Randolph, T. W. *Science* **1996**, *271*, 624−626.
(5) Lee, C. T.; Psathas, P. A.; Johnston, K. P. *Langmuir* **1999**, *15*, 6781−6791.
(6) Jacobson, G. B.; Lee, C. T.; Johnston, K. P. *J. Org. Chem.* **1999**, *64*, 1201−1206.
(7) Jacobson, G. B.; Lee, C. T.; daRocha, S. R. P.; Johnston, K. P. *J. Org. Chem.* **1999**, *64*, 1207−1210.
(8) Jacobson, G. B.; C. Ted Lee, J.; Johnston, K. P.; Tumas, W. *J. Am. Chem. Soc.* **1999**, *121*, 11902−11903.
(9) Ji, M.; Chen, X.; Wai, C. M.; Fulton, J. L. *J. Am. Chem. Soc.* **1999**, *121*, 2631−2632.
(10) Holmes, J. D.; Bhargava, P. A.; Korgel, B. A.; Johnston, K. P. *Langmuir* **1999**, *15*, 6613−6615.
(11) Yeung, L. K.; Lee, C. T.; Johnston, K. P.; Crooks, R. M. *Chem. Commun.* **2001**, 2290−2291.
(12) Yates, M. Z.; Apodaca, D. L.; Campbell, M. L.; Birnbaum, E. R.; McCleskey, T. M. *Chem. Commun.* **2001**, 25−26.
(13) Fremgen, D. E.; Smotkin, E. S.; Rex E. Gerald, I.; Klingler, R. J.; Rathke, J. W. *J. Supercrit. Fluids* **2001**, *19*, 287−298.
(14) Lee, D.; Hutchison, J. C.; DeSimone, J. M.; Murray, R. W. *Abstracts of Papers*, 222nd National Meeting of the American Chemical Society, Chicago, IL, August 26−30, 2001; American Chemical Society: Washington, DC, 2001; p. COLL-142.
(15) Ghenciu, E. G.; Russell, A. J.; Beckman, E. J. *Biotechnol. Bioeng.* **1998**, *58*, 572−580.
(16) Holmes, J. D.; Steytler, D. C.; Rees, G. D.; Robinson, B. H. *Langmuir* **1998**, *14*, 6371−6376.
(17) Kane, M. A.; Baker, G. A.; Pandey, S.; Bright, F. V. *Langmuir* **2000**, *16*, 4901−4905.
(18) Butler, R.; Davies, C. M.; Cooper, A. I. *Adv. Mater.* **2001**, *13*, 1459−1463.
(19) Hoefling, T. A.; Enick, R. M.; Beckman, E. J. *J. Phys. Chem.* **1991**, *95*, 7127−7129.
(20) Lee, C. T.; Johnston, K. P.; Dai, H. J.; Cochran, H. D.; Melnichenko, Y. B.; Wignall, G. D. *J. Phys. Chem. B* **2001**, *105*, 3540−3548.
(21) Eastoe, J.; Cazalles, B. M. H.; Steytler, D. C.; Holmes, J. D.; Pitt, A. R.; Wear, T. J.; Heenan, R. K. *Langmuir* **1997**, *13*, 6980−6984.
(22) Liu, Z.-T.; Erkey, C. *Langmuir* **2001**, *17*, 274−277.
(23) Lee, C. T.; Johnston, K. P.; Dai, H. J.; Cochran, H. D.; Melnichenko, Y. B.; Wignall, G. D. *J. Phys. Chem. B* **2000**, *104*, 11094−11102.
(24) Singey, E. J.; Liu, W.; Beckman, E. J. *Fluid Phase Equilib.* **1997**, *128*, 199−219.
(25) Diep, P.; Jordan, K. D.; Johnson, J. K.; Beckman, E. J. *J. Phys. Chem. A* **1998**, *102*, 2231−2236.
(26) Eastoe, J.; Paul, A.; Nave, S.; Steytler, D. C.; Robinson, B. H.; Rumsey, E.; Thorpe, M.; Heenan, R. K. *J. Am. Chem. Soc.* **2001**, *123*, 988−989.

and W/C emulsions[27] have been formed with AOT analogues that have a high degree of methyl branching and thus have favorable CO_2−surfactant interactions.[28]

In contrast, the formation of water-continuous dispersions of supercritical fluids requires water-soluble surfactants containing surfactant tails with enough hydrophobicity to aggregate and form micelles in water.[29] For example, supercritical xenon and ethylene solubilized in aqueous SDS micelles have been studied by steady-state fluorescence[30] and by SAXS.[31] Fluorocarbon surfactant tails are more hydrophobic than their hydrocarbon counterparts, favoring the formation of stable fluorocarbon micelles and fluorocarbon oil-in-water microemulsions.[32]

Recently, CO_2-in-water (C/W) macroemulsions have been formed with fluorocarbon[5,33] and hydrocarbon[34] surfactants; however, C/W microemulsions have not been reported. The solubilization of dense CO_2 with both ionic[35] and nonionic[36] hydrocarbon surfactants has been attempted, but did not lead to the formation of C/W microemulsions, as evidenced by minimal micelle growth of less than 2% with less than 0.35 mol % of CO_2 in the micelle. The limited growth was due to the relatively low affinity of CO_2 for the hydrocarbon surfactant tails. Perfluoropolyether-based carboxylate surfactants have been shown to form a variety of structures in water, including micelles and liquid-crystalline phases.[37−39] Because CO_2 is completely miscible with PFPE-based surfactants in this molecular weight range,[40] aqueous PFPE micelles are likely to swell substantially with addition of CO_2.

The objective of this study is to swell micelles in water to form C/W microemulsions and to employ these microemulsions to solubilize compounds that are fluorophobic but CO_2-philic. We use dynamic light scattering (DLS) to study the effect of the addition of CO_2 on the size and shape of micelles formed by 3 wt % perfluoropolyether potassium carboxylate surfactant (MW = 608 g/mol) in water. The pressure and temperature are varied for a given overall composition to cause changes in partitioning of CO_2 between the microemulsion droplets and the continuous phase. A geometric model and surfactant packing argument is applied to analyze the DLS results for the micelle size and shape and is further supported by TEM images of frozen surfactant solutions. UV−vis spectroscopy is used to measure the increase in micellar solubilization of the fluorophobic probe pyrene as CO_2 swells the micelles, similarly to recent studies on environmentally benign CO_2-swollen fluorous solvents.[41] Steady-state fluorescence measurements provide insight into the location of low concentrations of pyrene and $(dansyl)_2$PFPE probes upon addition of CO_2 to the micelles.

Experimental Section

Materials. A potassium carboxylate perfluoropolyether (PFPE-K) surfactant of the form

$$CF_3-(O-CF_2-CF(CF_3))_n-(O-CF_2)-COO^-K^+$$

was synthesized from the carboxylic acid (Ausimont, lot no. 0528 RB, MW_{avg} = 570 g/mol) by reaction with excess potassium hydroxide and subsequent purification by extraction into methanol. Full conversion was assured by noting the disappearance of the −COOH peak at 1780 cm^{-1} with FT-IR spectroscopy (Perkin-Elmer). Gas chromatography revealed that the polydisperse PFPE acid consisted of two primary fractions. Approximately 5% of the sample was evidently unfunctionalized fluorocarbon that could be reduced to ca. 0.05% (based on GC areas) by extraction with methanol and centrifugation of aqueous solutions to remove larger aggregates. However, the appearance of these large aggregates in aqueous solution could never be totally eliminated (see the discussion of the light-scattering results). Pyrene (Aldrich, 99%, optical grade) was used as received. The fluorophilic probe $(dansyl)_2$PFPE (**I**) was prepared by the reaction of tetrahydroperfluoropoly(ethylene glycol), $HOCH_2CF_2O(CF_2CF_2O)_nCF_2CH_2OH$, which was produced by the direct fluorination of the methyl ester of poly(ethylene glycol) (Aldrich, MW ca. 600) as previously described,[42] with an excess of dansyl chloride (Aldrich) and two equivalents of pyridine in tetrahydrofuran at room temperature for 72 h. The final product was then extracted into 1,1,2-trichlorotrifluoroethane (Aldrich), washed with a saturated sodium chloride solution, and vacuum-stripped. The final product was characterized with UV−vis and mass spectroscopy ($10 \le n \le 20$; $n = 14$ most abundant). Instrument grade CO_2 (Praxair) passed through a trap (Oxiclear, model no. RGP-R1-300) and Nanopure II water (Barnstead) were used throughout.

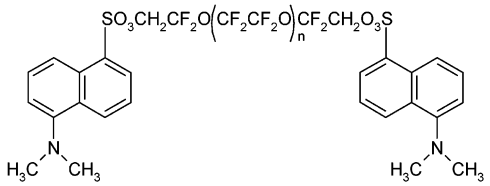

(I)

Phase Behavior Measurements. PFPE-K solutions in water were prepared with the desired amount of carbon dioxide in a high-pressure, variable-volume view cell equipped with a sapphire window that permitted visual observation of the phase behavior.[40] A piston inside the view cell was used to vary the pressure independently of the temperature, which was controlled with a water bath (±0.1 °C). System pressure was controlled with a computer-controlled syringe pump (Isco 260D) to within 1 bar by using CO_2 as the pressurizing fluid on the backside of the piston. The cell contents were mixed with a magnetic stir bar.

Dynamic Light Scattering. Micellar solutions were circulated from the phase-behavior cell to a specially designed light-scattering cell with a reciprocating minipump (Thermal Separations Products) through a 0.5-μm high-pressure filter (Alltech), as shown in Figure 1. The cylindrical light-scattering cell had HEMLUX sapphire windows

(27) Johnston, K. P.; Cho, D.; da Rocha, S. R. P.; Psathas, P. A.; Ryoo, W. S.; Webber, S. E.; Eastoe, J.; Dupont, A.; Steytler, D. C. *Langmuir* **2001**, *17*, 7191−7193.
(28) Fink, R.; Hancu, D.; Valentine, R.; Beckman, E. J. *J. Phys. Chem. B* **1999**, *103*, 6441−6444.
(29) Tanford, C. *The Hydrophobic Effect: Formation of Micelles and Biological Membranes*, 2nd ed.; Wiley-Interscience Publications: New York, 1980.
(30) Zhang, J.; Fulton, J. L. ACS Symposium Series 608; American Chemical Society: Washington, DC, 1995; pp. 111−125.
(31) Fulton, J. L. In *Handbook of Microemulsion Science and Technology*; Kumar, P., Mittal, K. L., Eds.; Marcel Dekker: New York, 1999; pp. 629−650.
(32) Kunieda, H.; Shinoda, K. *J. Phys. Chem.* **1976**, *80*, 2468−2470.
(33) Ghenciu, E. G.; Beckman, E. J. *Ind. Eng. Chem. Res.* **1997**, *36*, 5366−5370.
(34) da Rocha, S. R. P.; Harrison, K. L.; Johnston, K. P. *Langmuir* **1999**, *15*, 419−428.
(35) Oates, J. D.; Schechter, R. S. *J. Colloid Interface Sci.* **1989**, *131*, 307−319.
(36) Zielinski, R. G.; Kaler, E. W.; Paulaitis, M. E. *J. Phys. Chem.* **1995**, *99*, 10354−10358.
(37) Monduzzi, M. *Curr. Opin. Colloid Interface Sci.* **1998**, *3*, 467−477.
(38) Monduzzi, M.; Chittofrati, A.; Boselli, V. *J. Phys. Chem.* **1994**, *98*, 7591−7598.
(39) Caboi, F.; Chittofrati, A.; Lazzari, P.; Monduzzi, M. *Colloids Surf. A* **1999**, *160*, 47−56.
(40) Lee, C. T.; Bhargava, P.; Johnston, K. P. *J. Phys. Chem. B* **2000**, *104*, 4448−4456.
(41) Hallett, J. P.; West, K. N.; Brown, J.; Bush, D.; Liotta, C. L.; Eckert, C. A. In *AIChE Annual Meeting*; Reno, NV, 2001.
(42) Psathas, P. A.; Sander, E. A.; Ryoo, W.; Mitchell, D.; Lagow, R. J.; Lim, K. T.; Johnston, K. P. *J. Dispersion Sci. Technol.* **2002**, *23*, 81−91.

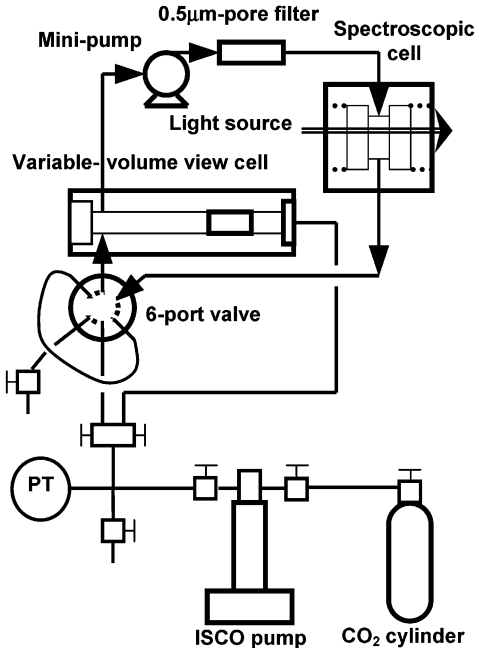

Figure 1. Schematic representation of the high-pressure DLS apparatus.

(Crystal Systems, 0001 orientation) (2.54 cm diameter × 0.70 cm thickness) secured at both ends with threaded stainless steel caps, as previously described,[27] resulting in a path length of 0.7 cm. The surfaces of light-scattering cell were finished with black oxide (Fe_3O_4) to minimize the reflection of light within the cell. The insulated light-scattering cell was temperature-controlled with cartridge heaters (Omega), while the recirculation lines were jacketed with water from the phase-behavior cell water bath, resulting in temperature control to within 0.2 °C.

Two strategies were employed for the DLS measurements. In the first type, a fixed amount of CO_2 (7 wt % based on the mass of water) was added to a 3 wt % PFPE-K solution, and this composition was used throughout the experiment. In the second type, controlled amounts of CO_2 were added to a 3 wt % PFPE-K solution at 35 °C and either 211 or 348 bar using a 200-μL sample loop connected to the six-port valve (Valco), followed by stirring and recirculation. Each injection increased the CO_2 concentration by 1.5 wt %. These titration measurements were performed until the solution became hazy and eventually underwent phase separation. The micelle size in the CO_2-free solution at 35 °C under atmospheric pressure was measured prior to CO_2 injection.

It was verified that neither excluded volume effects nor electrostatics significantly influenced the DLS behavior of the micelles in pure water. Varying the PFPE-K concentration from 0.2 wt % to 5 wt % changed the average diffusion coefficient of the small particles from 8.0×10^{-11} m^2/s to 7.0×10^{-11} m^2/s, which is within experimental error. Likewise, adding KCl up to 40 mM decreased the diffusion coefficient by ca. 15%, as is typical for surfactant micelles.[43,44] There was a negligible effect from a small population of large particles in all of these experiments (see below).

The coherent light source was a 17-mW He−Ne laser (Melles Griot, $\lambda = 632.8$ nm) mounted on a custom-built goniometer along with the light-scattering cell. The dynamic light-scattering measurements were taken with a Brookhaven BI-9000AT digital autocorrelator with 522 real-time channels. The scattered light signal was transmitted by an optical fiber coupled to a fiber collimator (SELFOC microlens, 0.25 pitch) and was detected by an avalanche photodiode. The true scattering angle was obtained from the external angle of the fiber optic by using Snell's law to account for the refraction of the scattered light at the window surfaces. The geometry of the light-scattering cell and the detection optics of the fiber allowed measurement of scattering angles less than 30° with an accuracy of ±5 min in arc.

Examination of the correlation functions revealed two relaxation processes with fast and slow decay rates of order 1000 and 100 s^{-1}, respectively. The former correspond to the PFPE-K micelles, while the latter could be the result of emulsification of unconverted fluorocarbon oil in the surfactant. To reduce the effect of impurities, the aqueous surfactant solutions were centrifuged for 1 h, passed through syringe filters (Gelman, PVDF, 0.2 μm), and circulated through an in-line filter. After these steps, the slow relaxation scattering intensity and the slow relaxation time constant decreased by 30 and 50%, respectively, without affecting the fast relaxation rate. Evidently the impurity is not particularly surface-active. However, even without filtration the volume fraction of the relatively large scatterers ($d_H \approx$ 200 nm) was negligibly small (less than 0.1 vol %), considering that the ratio of the intensity distribution to the volume fraction scales as radius to the third power.[45] Diffusion coefficients were determined using non-negative least squares (NNLS) software provided by Brookhaven. This analysis provides a distribution of hydrodynamic diameters based on the Stokes−Einstein relationship between diffusion coefficient and radius of a sphere ($D_0 = k_BT/3\pi\eta d_H$). The fit can be weighted by scattering intensity, by number density of scatterers, or by volume fraction of scatterers, which is our preferred approach. Each reported diffusion coefficient corresponds to the maximum of the distribution and is the average of four runs, with the standard deviation σ less than 5×10^{-12} m^2/s between runs.

Steady-State Fluorescence. The high-pressure fluorescence measurements were performed in a variable-volume view cell mounted vertically in a fluorometer and equipped with four 5/8 in. diameter × 3/16 in. thick sapphire windows at 90° intervals around the circumference, resulting in a path length of 22.3 mm.[34] The inner diameter of the view cell was 11/16 in., and the length was 11.7 cm. A magnetic stir bar inside the cell was used to mix the cell contents. System pressure was controlled with a manual syringe pump (High-Pressure Equipment Co.) to within 1 bar by using CO_2 as the pressurizing fluid on the backside of the piston, and system temperature was controlled to within ±0.2 °C with heating tape. The steady-state fluorescence measurements were performed on a SPEX DM3000 Fluorolog-τ2 spectrofluorometer equipped with a 450-W xenon light source, Czerny-Turner double monochromators for excitation and emission, and Hamamatsu R928-P emission and reference (rhodamine-B) photomultipliers. Pyrene (6×10^{-7} M) was excited at 334 nm, while $(dansyl)_2$PFPE (4×10^{-5} M) was excited at 284 nm.

UV−Vis Absorption Measurements. UV−vis spectra were measured by flowing the contents of the phase-behavior cell through a 0.5-μm high-pressure filter (Alltech) to a high-pressure spectroscopic cell with a reciprocating minipump (Thermal Separations Products). The spectroscopic cell consisted of two optical-grade sapphire windows forming a path length of 0.96 cm, as previously described.[46] Heating tape controlled the temperature of the UV−vis cell to within ±0.2 °C. The UV−vis spectra were recorded using a Cary 300 series dual-beam spectrophotometer (Varian).

Transmission Electron Microscopy on Freeze-Dried Sample of PFPE-K Solution. The morphology of CO_2-free micelles was determined by TEM to interpret the DLS data. Aqueous solutions of PFPE-K (3 wt %) and of uranyl acetate (2% w/v) were consecutively applied on a 200 mesh copper EM grid. After removal of excess sample and stain by touching the grid edge to filter paper, the sample grid was quickly transferred into a 20-mL vial containing liquid nitrogen. The

(43) Sushkin, N. V.; Clomenil, D.; Ren, J.; Phillies, G. D. J. *Langmuir* **1999**, *15*, 3492−3498.
(44) Mishic, J. R.; Fisch, M. R. *J. Chem. Phys.* **1990**, *92*, 3222−3229.
(45) Hallett, F. R.; Craig, T.; Marsh, J.; Nickel, B. *Can. J. Spectrosc.* **1989**, *34*, 63−70.
(46) Clarke, M. J.; Harrison, K. L.; Johnston, K. P.; Howdle, S. M. *J. Am. Chem. Soc.* **1997**, *119*, 6399−6406.

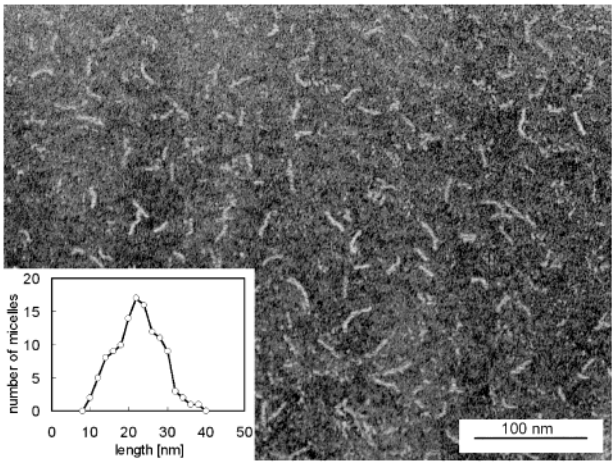

Figure 2. TEM image of a freeze-dried 3 wt % aqueous solution of PFPE-K. Inset is the distribution of cylindrical micelle lengths obtained by direct measurement from the image.

vial was placed in a vacuum freeze-drier kept below 200 K before the liquid nitrogen was completely evaporated. The TEM image was taken using a Philips EM208 at 89 kV after 24 h of freeze-drying. A distribution of cylindrical micelles was observed (Figure 2) with an average length of 22.4 ± 5.8 nm. Similar lengths were obtained from TEM images using a 0.3 wt % solution of PFPE-K.

Results and Discussion

Dynamic Light-Scattering Studies and Phase Stability. The micelle diffusion coefficients in water as a function of temperature and CO_2 pressure are given in Table 1. Decreasing the pressure generally results in a decrease in micelle diffusion coefficient, indicating an increase in micelle size. As will be discussed in detail later, this is because, as the CO_2 pressure is decreased, the amount of CO_2 dissolved in bulk water is diminished and more CO_2 is available to partition into the PFPE micelle. Analysis of these diffusion coefficients using the Stokes−Einstein equation for spherical particles gives micelle hydrodynamic diameters (d_H) ranging between 10 nm (no added CO_2) and 80 nm. It is generally accepted that the maximum dimension for the diameter of a spherical micelle is twice the surfactant tail length plus twice the Stern layer of hydrated surfactant ions and counterions. The length of the perfluoropolyether tail of this surfactant has been measured by SANS to be approximately 1.1 nm,[20] and the thickness of the Stern layer is generally less than 0.5 nm. These values are similar to those reported for SDS micelles in water.[47] Thus, the d_H of 10 nm cannot correspond to spherical micelles.

TEM images show that the CO_2-free micelles are cylindrical (Figure 2). The change in shape of rodlike micelles upon solubilization varies with the nature of the solubilizate.[48] For example, this behavior has been investigated for the surfactant hexadecyltrimethylammonium bromide (C_{16}TAB). For long-chain alkanes ($> C_8 - C_{10}$), where the beneficial free energy of mixing between the oil and the surfactant tails is low, an inner core of solubilizate will often develop. In this case, the diameter of the rodlike micelles will grow to a value considerably larger than twice the tail length. For shorter alkanes, however, the free energy of mixing between the oil and the surfactant tails is large,

Table 1. Results of the DLS Experiments Performed on CO_2-Swollen Fluorocarbon Micelles in Water in the One-Phase Region[a]

T (°C)	P (bar)	R_{CO2}	D_{app} (/10^{11} m^2/s)	L (nm)	p
25	350	–	5.31	21.1	0.367
25	315	0.13	5.21	21.8	0.383
25	281	0.75	4.87	24.3	0.400
25	246	1.43	5.16	22.1	0.413
25	211	2.15	4.67	26.0	0.430
25	176	2.94	4.85	24.5	0.443
25	141	3.80	4.54	27.2	0.459
25	107	5.47	4.46	28.0	0.473
25	89	5.47	3.72	37.1	0.487
25	72	6.12	3.48	41.0	0.496
35	350	2.26	6.97	20.2	0.427
35	314	2.89	6.06	25.4	0.443
35	281	3.52	5.61	28.8	0.455
35	246	4.22	5.08	33.6	0.468
35	212	4.98	5.36	30.9	0.477
35	177	5.81	4.60	39.0	0.491
35	142	6.77	3.99	48.2	0.505
35	107	7.92	3.66	54.6	0.518
50	349	4.59	6.40	38.5	0.476
50	315	5.27	6.50	37.6	0.484
50	281	6.00	6.70	35.9	0.492
50	246	6.81	5.91	43.3	0.504
50	212	7.69	5.34	50.3	0.515
50	205	7.88	5.18	52.5	0.517
50	198	8.07	4.83	58.1	0.520
50	191	8.27	4.27	69.1	0.524
75	350	6.12	8.43	49.4	0.498
75	315	6.97	7.71	56.2	0.509
75	281	7.88	5.87	82.3	0.521

[a] Diffusion coefficients calculated from the fast relaxation process by NNLS. R_{CO2} calculated by assuming water saturated by CO_2. L determined from eq 1 with $d = 3.2$ nm.

and generally a discrete oil core will not be formed. In this case, the cylindrical micelles grow longer without a change in radius. We have previously found complete miscibility of CO_2 and the PFPE surfactant.[40] Therefore, it is reasonable to assume that the free energy of CO_2 and PFPE mixing is favorable and that growth of the cylindrical micelles in the axial direction without an increase in diameter may be expected.

The micelle dimensions were obtained from the expression of the infinite dilution diffusion coefficient D_0 of a cylinder of length L and diameter d given by Tirado and de la Torre[49,50] for $2 \leq L/d \leq 30$

$$D_0 = \frac{k_B T[\ln(\zeta) + \gamma]}{3\pi\eta L} \quad (1)$$

where k_B is the Boltzmann constant, T is the temperature, $\zeta = L/d$, η is solvent viscosity, and $\gamma = 0.312 + 0.565/\zeta - 0.1/\zeta^2$. The results of this calculation, assuming a micelle diameter of 3.2 nm (based on the discussion above), are plotted in Figure 3 versus the molar ratio of CO_2 to surfactant. The value of L as R_{CO2} approaches zero is in good agreement with the TEM image in Figure 2. This molar ratio was determined as follows. The micelles were formed by adding 3.0 wt % PFPE-K surfactant and 7.0 wt % CO_2 to water. The solubility of CO_2 in water decreases as the temperature is increased or the pressure is decreased. We assume that the CO_2 present in the system first

(47) Arleth, L.; Bergstroem, M.; Pedersen, J. S. *Langmuir* **2002**, *18*, 5343−5353.
(48) Törnblom, M.; Henriksson, U. *J. Phys. Chem. B* **1997**, *101*, 6028−6035.
(49) Tirado, M.; Garcia de la Torre, J. *J. Phys. Chem.* **1979**, *71*, 2581.
(50) Tirado, M.; Garcia de la Torre, J. *J. Phys. Chem.* **1980**, *73*, 1986.

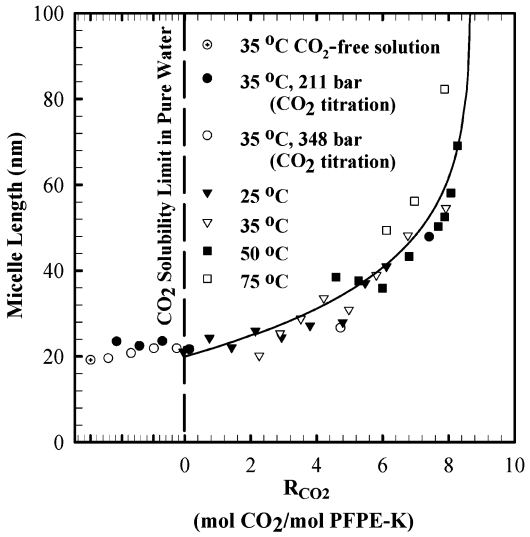

Figure 3. Micelle length determined from DLS versus R_{CO2}, the molar ratio of CO_2 to surfactant, in the micelle. The R_{CO2} value is determined by subtracting the CO_2 solubility in pure water from the total amount of CO_2 in the system (2.98 mol %) (see text). The experimental points for R_{CO2} less than zero are ordered according to the pressure. The line is based on geometric modeling (eq 4 and regressed a_H).

saturates the water, with any excess going into the micelles. Any excess from the micelles causes phase separation. Thus, the amount of CO_2 in excess of the aqueous solubility limit, i.e., the amount of CO_2 dissolved in the micelles, may be increased by decreasing the pressure or by increasing temperature at a fixed total amount of CO_2 in a one-phase system. The amount of CO_2 solubilized in the micelles may be determined by subtracting the CO_2 solubility in pure water from the total amount of CO_2. For example, the solubility of CO_2 in water is approximately 7.0 wt % at 25 °C and 345 bar and 5.4 wt % at 50 °C and 191 bar.[23,51,52] Therefore, the molar ratio R_{CO2} may be varied from 0 at 25 °C and 345 bar to 8.27 at 50 °C and 191 bar, assuming a one-phase system. The *x*-axis in Figure 3 is then the molar ratio of CO_2 to surfactant in the micelle, R_{CO2}. For a given pressure, R_{CO2} increases as temperature increases due to the lower solubility of CO_2 in bulk water. At low temperature and high pressure, all of the CO_2 dissolves in bulk water and R_{CO2} goes to zero. All points to the left of the CO_2 saturation line are ordered according to the CO_2 pressure, since R_{CO2} is unknown.

Note that these R_{CO2} values represent the minimum possible CO_2-to-surfactant ratio in the micelles. If the CO_2 does not saturate the bulk water before going into the micelles, then R_{CO2} will be larger. Saturation of the bulk water has often been verified for the partitioning of an oil between micellar and bulk-water domains and is reasonable for our system, certainly at larger values of R_{CO2}.[53]

To test the validity of assuming CO_2-saturated water, a series of CO_2 titration experiments were performed in which small amounts of CO_2 were added incrementally to the micellar solution while checking for micellar growth as the aqueous solubility limit was approached. As seen in Table 2, the measured diffusion coefficients were not much smaller than

Table 2. Results of DLS Experiments Performed by CO_2 Titration[a]

T (°C)	*P* (bar)	wt % CO_2	D_{app} ($/10^{11}$ m^2/s)	R_{CO2}	*L* (nm)
35	1.01	0.0	7.17	–	19.2
35	211	1.5	6.35	–	23.5
35	211	3.0	6.53	–	22.5
35	211	4.5	6.34	–	23.6
35	211	6.0	6.67	0.14	21.7
35	211	7.5	4.00	7.41	47.9
35	348	1.5	7.09	–	19.6
35	348	3.0	6.84	–	20.8
35	348	4.5	6.63	–	21.9
35	348	6.0	6.64	–	21.9
35	348	7.5	5.88	4.72	26.7

[a] Diffusion coefficients calculated from the fast relaxation process by NNLS. R_{CO2} calculated by assuming water saturated by CO_2. *L* determined from eq 1 with $d = 3.2$ nm.

those for the CO_2-free micelles ($P = 1$ atm) and agree with the limiting values at the lowest R_{CO2}, supporting our assumption that water is very nearly saturated with CO_2 even in the presence of the micelles. For both conditions in Table 2, addition of a final aliquot of CO_2 resulted in a hazy solution and eventual phase separation after several hours, producing a small bubble of CO_2. Note that in each case, dissolution of this final aliquot of CO_2 would require R_{CO2} values greater than 8, which seems to be the maximum R_{CO2} obtainable (see Figure 3).

As seen in Figure 3, the micelle length increases from about 20 nm at low values of R_{CO2} to nearly 80 nm at the highest R_{CO2} values investigated. Thus, the micelle volume increases from 146 Å^3 (7.3% in the spherical caps) to 628 Å^3 (1.7% in the caps). This 330% increase in micelle size upon the addition of CO_2 to PFPE-K micelles in water is dramatic, especially in contrast to the low amounts of CO_2 solubilized in hexaethylene glycol monododecyl ether ($C_{12}E_6$) micelles in water, as evidenced by the small change in micelle size (within SANS experimental error).[36] Furthermore, the R_{CO2} values obtained here are 25 times greater that those obtained by the addition of dense CO_2 to sodium dodecyl sulfate (SDS) micelles in water.[35] These results demonstrate the CO_2-philicity of the PFPE tails.

Micelle growth upon addition of a solute (oil) is controlled by the balance between the beneficial free energy of mixing of the oil with the surfactant tails and the free energy penalty required to change the micelle size and shape.[35] The free energy penalty upon micelle growth and elongation results from the increase in the interfacial area that must be stabilized. The free energy of mixing between CO_2 and fluorocarbon surfactant tails is significantly more favorable than that between CO_2 and hydrocarbon tails.[35] For example, a 672 g/mol fluorinated poly(propylene oxide) (i.e., perfluoropolyether) *ionic* surfactant is completely miscible with CO_2,[40] while the solubility of 2000 g/mol poly(propylene oxide) in CO_2 is only 0.5 wt % at 35 °C and 207 bar.[54] Therefore, the favorable free energy of mixing of CO_2 with the fluorocarbon surfactant tails in this study counterbalances the unfavorable free energy penalty upon micelle growth and elongation more effectively than in the case of hydrocarbon surfactants.

The amount of CO_2 solubilization into the micelles that results in phase separation was independent of temperature from 35 to

(51) Wiebe, R.; Gaddy, V. L. *J. Am. Chem. Soc.* **1939**, *61*, 315−318.
(52) Wiebe, R.; Gaddy, V. L. *J. Am. Chem. Soc.* **1940**, *62*, 815−817.
(53) Dunaway, C. S.; Christian, S. D.; Scamehorn, J. F. In *Solubilization in Surfactant Aggregates*; Christian, S. D., Scamehorn, J. F., Eds.; Marcel Dekker: New York, 1995.
(54) O'Neill, M. L.; Cao, Q.; Fang, M.; Johnston, K. P.; Wilkinson, S. P.; Smith, C. D.; Kerschner, J. L.; Jureller, S. H. *Ind. Eng. Chem. Res.* **1998**, *37*, 3067−3079.

75 °C with a maximum R_{CO2} of about 8, while the maximum R_{CO2} value at 25 °C was slightly greater than 6. In addition, the nature of the cloud points was observed to be different in these two temperature regions. The cloud point for each temperature was approximately 10 bar below the lowest pressure listed in Table 1. At 25 °C, the cloud point was evidenced by the formation of a very small CO_2 bubble in a clear microemulsion phase. For 35−75 °C, however, a sharp increase in haziness of the solutions was observed at the cloud point, with very long times required for phase separation (no discernible change in scattering intensity for more than 2 h). Two separate phenomena must be responsible for these widely different observations of phase separation. The bubble-type cloud point at 25 °C and pressures below 72 bar is likely the result of the vapor−liquid transition in pure CO_2, which has a vapor pressure of 64 bar at 25 °C. Note that it was difficult to measure cloud points with high accuracy due to the pressure pulses produced by the minipump (±7 bar). The cloudiness observed in the phase transitions at 35−75 °C, however, suggest the formation of surfactant structures with domain sizes approaching the wavelength of light. This system was observed to cycle from cloudy to clear with each minipump stroke at the lowest pressures listed in Table 1, suggesting a rapid and reversible phase transition.

A simple geometric model may provide further insight into the behavior of Figure 3 and the nature of the high-temperature phase transitions. The micelles may be considered as cylinders of length l capped with hemispheres of diameter d. Thus, the ratio of micelle volume to surface area is given by

$$\frac{V}{A} = \frac{d}{12}\left(\frac{3L - d}{L}\right) \tag{2}$$

where L is the total micelle length ($l + d$) reported above and d is 3.2 nm. On the basis of an assumption of ideal mixing between surfactant tails and CO_2 molecules, we can also calculate V/A from the volumes of the micelle constituents by

$$\frac{V}{A} = \frac{n_c v_c + n_s v_s}{n_s a_H} = \frac{1}{a_H}(v_c R_{CO2} + v_s) \tag{3}$$

where n_c and n_s are the number density of CO_2 and surfactant molecules in the micelle with molecular volumes of v_c and v_s, respectively, and a_H is the area per surfactant molecule headgroup. The second part of eq 3 is an approximation, made because our surfactant concentration of 3 wt % (ca. 50 mM) was far above the cmc, which is less than a few mM for anionic PFPE surfactants.[55] Thus, the amount of the free surfactant dissolved in water is negligible. The molecular volume of surfactant is the sum of the volume of the headgroup and the PFPE tail ($v_s = v_{head} + v_{tail}$), where $v_{head} = 402$ Å^3 (COO^- hydrated radius from,[56] K^+ hydrated radius from[57]) and $v_{tail} = 490$ Å^3 from the density (1.8 g/mL) of PFPE oil.[58] Comparing eqs 2 and 3 gives

$$L = \frac{d}{3 - \frac{12}{a_H d}(v_c R_{CO2} + v_s)} \tag{4}$$

where a_H is the only unknown value. Since we assume that all of the CO_2 is mixed with the surfactant tails and does not form a pure CO_2 unmixed region, we use a liquidlike density of 1 g/mL to calculate v_c of CO_2. This value has been confirmed previously for CO_2 dissolved in condensed phases such as polymers.[59] From the measured values of L, the approximate equation $a_H = 8.76(R_{CO2}) + 118$ [Å^2] ($R^2 = 0.999$) is obtained from a regression of the micelle lengths according to eq 4, as shown in Figure 3. The a_H value of 118 Å^2 for $R_{CO2} = 0$ agrees nicely with those obtained for these PFPE surfactants at the planar CO_2−water interface ($a_H \approx 100$ Å^2)[34] and in W/C microemulsions ($a_H \approx 110$ Å^2).[23]

The a_H increase with R_{CO2} demonstrates the CO_2 swelling of the micelle. The adsorption of PFPE surfactants at the water−CO_2 interface has been described theoretically and experimentally.[60] The area per surfactant molecule at the water−CO_2 interface is much larger than that at a water−PFPE oil interface due to the differences in the interfacial tensions for the binary systems (without surfactant) and solvent penetration into the tail region. Therefore, as R_{CO2} increases, the area per surfactant molecule at the interface increases, thereby increasing a_H.

From these a_H values we calculate the surfactant packing parameter ($p = v/a_H l_T$), the ratio of the volume occupied by a surfactant molecule plus dissolved CO_2 ($v = v_s + R_{CO2} v_c$) to the product of the surface area per surfactant molecule times the surfactant tail length, as given in Table 1. The packing parameter is a measure of the interfacial curvature and increases from spherical ($p < 1/3$) to cylindrical ($1/3 < p < 1/2$) to planar ($1/2 < p$) geometries. For the R_{CO2} values obtained in this study, the packing parameters are generally in the cylindrical micelle regime, in support of our model. At each temperature, increased solubilization of CO_2 into the micelles results in an increase in the packing parameter, i.e., a less-curved interface, as expected due to the additional volume from CO_2 on the tail side of the interface. At 35−75 °C, a packing parameter of $p = 0.521 \pm 0.003$ is obtained just prior to phase separation, indicating that the observed cloud points in this temperature range could be the result of a cylindrical-to-lamellar phase transition that results in precipitation. This type of transition would be consistent with increased cloudiness as the cylindrical micelles aggregate and begin to form lamellar layers and is likely responsible for the sharp increase in measured micelle length observed at $R_{CO2} \approx 8$. Note that at 35−75 °C, the maximum packing parameters correspond to an increase in the volume occupied by each surfactant tail (plus solvation by CO_2) from 490 Å^3 at $R_{CO2} = 0$ to 1075 Å^3 at $R_{CO2} = 8$.

As the micelle volume fraction ϕ increases, the diffusion of a micelle becomes influenced by the other micelles in solution. Hence, the apparent, or measured, diffusion coefficient is given by $D_{app} = D_0 H(q)/S(q)$, where $H(q)$ represents the hydrodynamic interactions and $S(q)$ the thermodynamic (e.g., electrostatic) interactions. For spherical micelles, the first-order approximation yields[61] $D_{app} \approx D_0(1 + 1.56\phi)$, while the expression for cylindrical micelles is more complicated due to the parallel and

(55) Caporiccio, G.; Burzio, F.; Carniselli, G.; Biancardi, V. *J. Colloid Interface Sci.* **1984**, *98*, 202−209.
(56) Jorgensen, W. L.; Gao, J. *J. Phys. Chem.* **1986**, *90*, 2174−2182.
(57) Conway, B. E. *Ionic Hydration in Chemistry and Biophysics*; Elsevier: New York, 1981; Vol. 12.
(58) Chittofrati, A.; Boselli, V.; Visca, M.; Friberg, S. E. *J. Dispersion Sci. Technol.* **1994**, *15*, 711−726.
(59) Fleming, G. K.; Koros, W. J. *Macromolecules* **1986**, *19*, 2285−2291.
(60) da Rocha, S. R. P.; Johnston, K. P. *Langmuir* **2000**, *16*, 3690−3695.
(61) Long, M. A.; Kaler, E. W.; Lee, S. P.; Wignall, G. D. *J. Phys. Chem.* **1994**, *98*, 4402−4410.

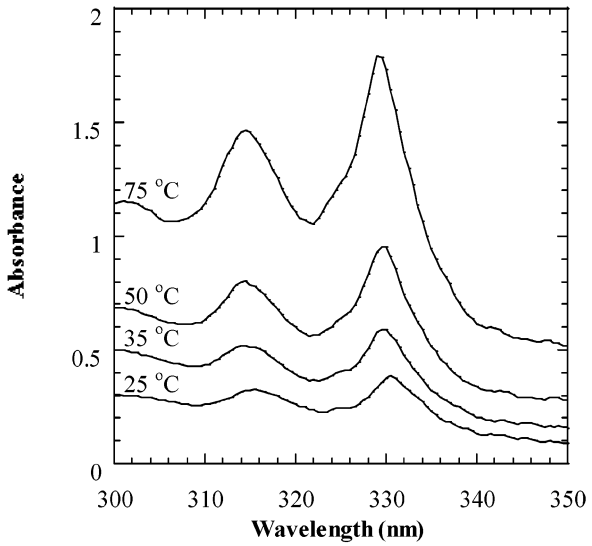

Figure 4. Absorption spectra for the pyrene-containing CO_2-swollen PFPE-K micelle system as a function of temperature at 345 bar.

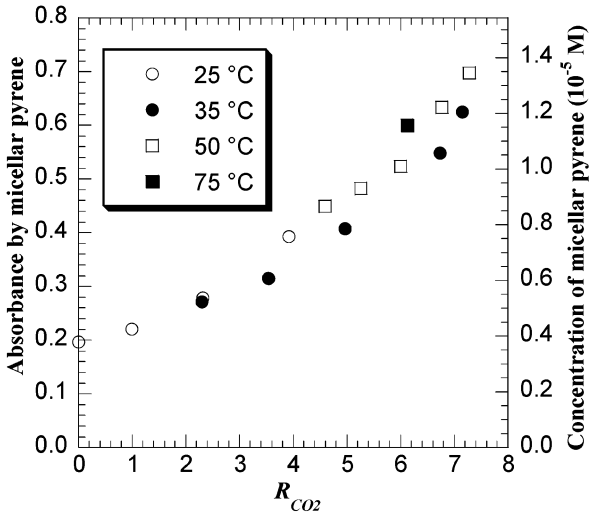

Figure 5. UV−vis absorbance and the corresponding solubility (based on total system volume) of pyrene in CO_2-swollen PFPE-K micelles versus R_{CO2}, the molar ratio of CO_2 to surfactant in the micelles. Only the contribution from micellar pyrene is included.

perpendicular components of the translational diffusion coefficient.[62,63] For the present study, the ϕ values can be estimated to be in the range of 0.017−0.036. Therefore, eq 1 can be used safely with $D_{app} \approx D_0$.

Spectroscopic Studies: Pyrene Uptake. To evaluate the potential of CO_2-swollen fluorocarbon micelles as solubilization agents, the solubility of pyrene was studied by UV−vis spectroscopy using the same surfactant and CO_2 concentrations as in Figure 3. Typical absorption spectra for the pyrene-containing CO_2-swollen micelle system are shown in Figure 4 as a function of temperature at 345 bar. The characteristic pyrene peaks at ca. 330, 315, and 300 nm are clearly evident, indicating a high degree of pyrene solubilization upon the addition of CO_2. The measured UV−vis spectra of pyrene in PFPE-K micelles in the absence of CO_2 showed an absorbance of 0.07 at the 330 nm peak, roughly twice that of pyrene in pure water (7×10^{-7} M, or an absorbance of ca. 0.04; $\epsilon = 5.4 \times 10^4$ cm^{-1} M^{-1}),[64] also at room temperature and with 1 cm path length. Similar results have been obtained with other fluorocarbon surfactants in water and has been attributed to the adsorption of pyrene at the micellar interface as opposed to inside the micelle cores, due to the relatively low affinity of pyrene for fluorocarbons, given the large difference in cohesive energy densities.[65−67]

As seen in Figure 4, increasing the temperature increases the absorbance, and hence the calculated solubility, of pyrene in the system. The primary reason for this solubility increase is the increase in micellar CO_2. Recall that, as the temperature is increased at constant pressure, the solubility of CO_2 in water decreases, resulting in an increase in the amount of CO_2 solubilized in the micelles. As the swollen micelles grow, they scatter more light, as evidenced by the increase in absorbance away from the pyrene peak, e.g., at 350 nm, in Figure 4. The contribution to the overall absorbance due to scattering was approximated using a spline and subtracted from the peak absorbance. Raising the temperature also has the effect of increasing the solubility of pyrene in bulk water. This was accounted for by subtracting the expected absorbance based on the volume fraction of the aqueous phase and literature values for the solubility of pyrene in bulk water at atmospheric pressure and the experimental temperature.[68] The overall effect is shown in Figure 5, which plots the net absorbance (i.e., the overall absorbance corrected for scattering from the micelles and for pyrene solubility in water) and the corresponding solubility (based on total system volume) of pyrene in the fluorocarbon micelles versus R_{CO2}. The raw absorbances, scattering corrections, and aqueous solubility corrections are available as Supporting Information. For comparison, the solubility of pyrene in bulk CO_2 is 2.1×10^{-3} M at 35 °C and 125 bar,[69] while the concentration of micellar pyrene at 35 °C and 128 bar ($R_{CO2} = 7.2$) is 1.21×10^{-5} M from Figure 5. On the basis of the volume fraction of CO_2 in the micellar solution ($\phi_{CO2} = 0.018$ at $\rho_{CO2} = 0.783$ g/mL), the maximum predicted solubility of pyrene in the micelles is 3.8×10^{-5} M if a pure CO_2 core were formed in the micelles. In other words, CO_2 in the fluorocarbon micelle core can solubilize approximately 31% (±2%) of the amount of pyrene dissolved in an equivalent volume of neat CO_2. This amount is substantial given that the volume ratio of micellar CO_2 to surfactant (∼1) is considerably below the molar ratio (R_{CO2}) value of 7.2. By swelling our micelles with CO_2 we observe an increase of the total solubility of pyrene by a factor of up to 10 over that in bulk water at the same temperatures.

This example demonstrates the ability to dissolve large amounts of lipophilic compounds into aqueous-phase fluorocarbon micelles upon the addition of CO_2. The reversibility of this solubilization upon removal of CO_2 pressure has potential advantages for recovery of solutes. Linear extrapolation to $R_{CO2} = 0$ gives a micellar pyrene concentration of $2.6 \pm 0.5 \times 10^{-6}$ M, which is over 4 times the value in room-temperature CO_2-free micelles. We believe that this difference is caused by

(62) Doi, M.; Shimada, T.; Okano, K. *J. Chem. Phys.* **1988**, *88*, 4070−4075.
(63) Maeda, T. *Macromolecules* **1989**, *22*, 1881−1890.
(64) Berlman, I. B. *Handbook of Fluorescence Spectra of Aromatic Molecules*, 2nd ed; Academic Press: New York, 1971.
(65) Weberskirch, R.; Preuschen, J.; Spiess, H. W.; Nuyken, O. *Macromol. Chem. Phys.* **2000**, *201*, 995−1007.
(66) Zhou, J.; Zhuang, D.; Yuan, X.; Jiang, M.; Zhang, Y. *Langmuir* **2000**, *16*, 9653−9661.
(67) Almgren, M.; Wang, K.; Asakawa, T. *Langmuir* **1997**, *13*, 4535−4544.
(68) Wauchope, R. D.; Getzen, F. W. *J. Chem. Eng. Data* **1972**, *17*, 38−41.
(69) Johnston, K. P.; Ziger, D. H.; Eckert, C. A. *Ind. Eng. Chem. Fundam.* **1982**, *21*, 191−197.

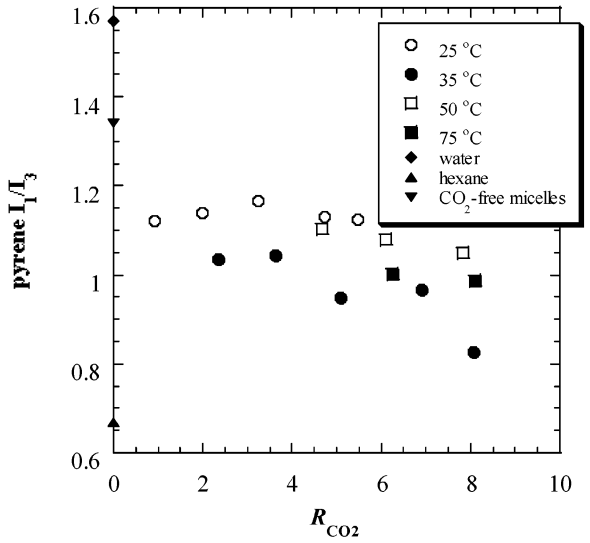

Figure 6. Pyrene I_1/I_3 versus the molar ratio of CO_2 dissolved in the micelles (R_{CO2}). The values for water, hexane, and CO_2-free micelles are for 25 °C.

preferential partitioning of CO_2 into the micelles. This effect is numerically significant only when the solubility limit of pure water is approached, i.e., $R_{CO2} < 3$, as evidenced by the slight change in slope around $R_{CO2} = 3$ in Figure 5.

Steady-state fluorescence measurements were performed to characterize the location of the solubilized pyrene in the fluorocarbon micelles. The fluorescence emission of pyrene is well documented, and the ratio of intensities of the first and third peaks, I_1/I_3, has been found to be a measure of the local polarity of the pyrene environment. For example, I_1/I_3 equals 1.59−1.87 in water, 0.6 in hexane, and 0.50 in perfluoromethylcyclohexane.[70,71] Figure 6 contains a plot of I_1/I_3 versus R_{CO2}, along with the values obtained for pyrene in water, in hexane, and in the fluorocarbon micelles before the addition of CO_2. An I_1/I_3 value of 1.35 for $R_{CO2} = 0$ is consistent with values obtained in other fluorocarbon micelles[65,66] and has been attributed to the solubilization of pyrene in a region of intermediate polarity between the water and fluorocarbon environments, i.e., the micellar interface. For the largest amount of CO_2 dissolved in the micelles, I_1/I_3 values of 0.8 to 1.0 are obtained. For comparison, I_1/I_3 is 0.9 for pyrene in neat CO_2 in the density range of this study.[72] As CO_2 swells and lengthens the micelles, pyrene is located in an increasingly nonpolar environment that is spectroscopically equivalent to pure CO_2. This result demonstrates that the additional pyrene dissolved in the fluorocarbon micelles upon the addition of CO_2 resides effectively in the micellar tail-CO_2 region. The low cohesive energy density of the PFPE tails would also give a low value of I_1/I_3 if the pyrene were soluble in the fluorocarbon core of the micelle. Therefore, incorporation of CO_2 into fluorocarbon micelles allows for the solubilization of relatively large amounts of fluorophobic hydrocarbons into the micellar core. Additionally, CO_2-swollen fluorocarbon micelle systems could be used to raise the solubility of fluorocarbon solutes in the aqueous phase.

Spectroscopic Studies: Dansyl Probe. To test the effect of CO_2 solubilization into fluorocarbon micelles on fluorophilic solutes, the fluorescence probe $(dansyl)_2$PFPE was employed. The dansyl group is another well-known polarity indicator, with a red-shift in the wavelength of maximum absorption (λ_{max}) as solvent polarity increases.[73] The λ_{max} values obtained for $(dansyl)_2$PFPE in the C/W microemulsions were 500 ± 2 nm, independent of the value of R_{CO2}. Here the temperature was varied from 25 to 75 °C, and the pressure, from 69 to 345 bar. These λ_{max} values are intermediate between those obtained in water ($\lambda_{max} = 516$ nm) and in the fluorocarbon solvent 1,1,2-trichlorotrifluoroethane ($\lambda_{max} = 483$ nm), and differ only slightly from the value obtained in CO_2-free PFPE-K micelles in water ($\lambda_{max} = 504$ nm). Thus, CO_2 does not appear to greatly affect the location of solubilization of this type of fluorophilic compound. Similarly to pyrene, the polar phenyl groups of dansyl are expected to preferentially partition to the micellar interface in the absence of CO_2. The perfluoropolyether linkage is solubilized in the micellar core and acts as a tether between the dansyl groups at the micelle interface. The inclusion of CO_2 in the micelles is not expected to affect the affinity of perfluoropolyether toward the micellar core but could result in a slight increase in the solubility of the dansyl groups in the micellar core. This solubility increase is expected to a much smaller extent than observed with pyrene because of the relatively polar groups in dansyl. Note that, although the location of the dansyl fluorophilic probe is unaffected by the addition of CO_2 to the micelles, the micellar growth and the increase in dispersed phase volume fraction that results from CO_2 solubilization would likely result in an increase in solubilization of the probe.

Solutions of CO_2 and water are acidic (pH = 3) due to the formation of carbonic acid and thus may protonate organic bases, such as the amine of the dansyl group ($pK_a \cong 3.5$).[74] The protonated dansyl species results in a second fluorescence peak. The wavelength of maximum emission of this peak was approximately 400 nm. Figure 7 shows the ratio of intensities of the neutral and protonated dansyl species, denoted here as I_n/I_p, as a function of R_{CO2} and temperature. At each temperature except 75 °C, the fraction of neutral dansyl slightly increases as the amount of CO_2 in the micelle increases. This observation suggests that CO_2 incorporation encourages the dansyl groups to move away from the interface, where they can come in contact with water and become protonated.

The I_n/I_p values in Figure 7 appear to be affected by temperature independently from R_{CO2}. Increases in temperature result in a decrease in I_n/I_p, or an increase in dansyl protonation. This temperature effect cannot be explained by acid−base reaction equilibrium, because the pK_a of the dansyl group is expected to decrease with increasing temperature, resulting in less dansyl protonation.[75] The pH of CO_2−water mixtures is relatively constant over the experimental temperature and pressure range employed here.[76]

We believe that the enhanced protonation of the dansyl group reflects its increased exposure to the aqueous phase. Our argument is as follows. Solubilization into micelles in water

(70) Kalyanasundaram, K.; Thomas, J. K. *J. Am. Chem. Soc.* **1977**, *99*, 2039−2044.
(71) Dong, D. C.; Winnik, M. A. *Can. J. Chem.* **1984**, *62*, 2560−2565.
(72) Brennecke, J. F.; Tomasko, D. L.; Peshkin, J.; Eckert, C. A. *Ind. Eng. Chem. Res.* **1990**, *29*, 1682−1690.
(73) Ren, B.; Gao, F.; Tong, Z.; Yan, Y. *Chem. Phys. Lett.* **1999**, *307*, 55−61.
(74) Strauss, U. P.; Vesnaver, G. *J. Phys. Chem.* **1975**, *79*, 1558−1561.
(75) Perrin, D. D. *Aust. J. Chem.* **1964**, *17*, 484−488.
(76) Holmes, J. D.; Ziegler, K. J.; Audriani, M.; Lee, C. T.; Bhargava, P. A.; Steytler, D. C.; Johnston, K. P. *J. Phys. Chem. B* **1999**, *103*, 5703−5711.

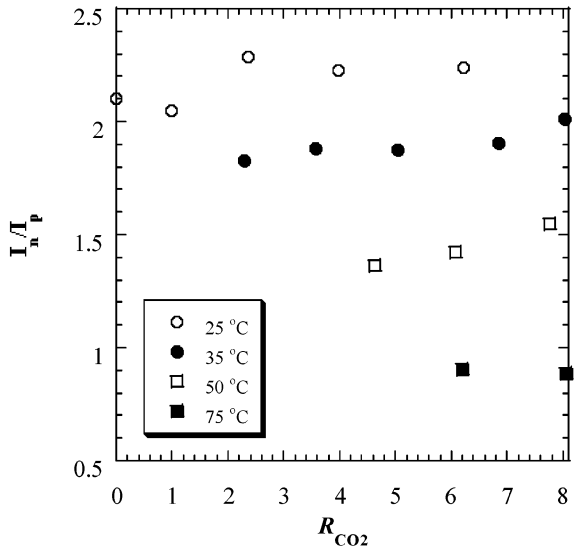

Figure 7. Ratio of intensities of the neutral and protonated dansyl species as a function of temperature and the amount of CO_2 dissolved in the micelles. Partitioning to the micellar interface results in increased protonation.

can generally be described with a two-site model involving the partitioning of the solute between the liquidlike core and the micellar interface.[77] For classical alkane-based micelles, nonpolar oils such as hexane reside exclusively in the micellar core region, while slightly polar oils, such as those containing aromatic rings, partition between the micelle core and the interface. The solubility of aromatics in water increases strongly with temperature. For example, the solubility of naphthalene in water increases 6-fold as the temperature increases from 25 to 65 °C.[78] Therefore, it is reasonable to expect that increasing the temperature results in an increase of the partitioning of the dansyl groups to the micellar interface, which is manifested by the increase in the degree of dansyl protonation seen in Figure 7.

Conclusions

The addition of dense (liquid or supercritical) CO_2 to perfluoropolyether micelles in water swells cylindrical, rodlike micelles to form for the first time CO_2-in-water (C/W) microemulsions. These microemulsions allow for the simultaneous solubilization of certain fluorophilic, lipophilic, and hydrophilic molecules. The cylindrical geometry for the microemulsions is consistent with the packing parameters in the range of 0.37−0.52 calculated from the area per surfactant molecule (a_H) values determined from the DLS measurements. By changing temperature or pressure or both to adjust the solubility of CO_2 in water, the molar ratio of CO_2 solubilized in the micelle to surfactant (R_{CO2}) can be tuned from 0 to 8, which increases the cylindrical micelle length from ca. 20 to 80 nm. The volume fraction of the micellar pseudophase increases from 0.017 without CO_2 to a maximum of 0.036. The increase in the area per surfactant headgroup with R_{CO2} is consistent with the much smaller interfacial tension between CO_2 and water versus fluoroethers and water, which lowers the surfactant adsorption. This type of large change in interfacial tension, and thus a_H, does not occur in solubilization of hydrocarbons into micelles with hydrocarbon tails. The light-scattering data always contained a small volume fraction of large particles ($d_H \approx 200$ nm) that is probably the result of unfunctionalized surfactant precursor acting as a chemical impurity. The CO_2-swollen fluorocarbon micelles can solubilize substantial amounts of fluorophobic molecules that are CO_2-philic. The maximum solubility of pyrene in the micelles is approximately 10 times higher than the solubility in bulk water and is about one-third of the solubility of pyrene expected in neat CO_2 based on the micelle volume fraction. The change of the polarity-sensitive pyrene fluorescence (I_1/I_3) versus R_{CO2} shows that addition of CO_2 to the micelles results in partitioning of pyrene from the interface to the tail-CO_2 region of the micelle core. At the highest R_{CO2} values, pyrene senses a polarity comparable to that of pure CO_2. Similarly, as R_{CO2} increases, the fluorophilic probe $(dansyl)_2$PFPE resides in a decreasingly polar environment, although this effect is much smaller than that observed for pyrene. The ability to form C/W microemulsions offers new opportunities in reaction, separation, and materials formation processes with two environmentally benign solvents, carbon dioxide and water.

Acknowledgment. This material is based upon work supported by the STC Program of the National Science Foundation under Agreement No. CHE-9876674, by the Texas Advanced Technology Program, by the Welch Foundation (K.P.J. F-1319 and S.E.W. F-356), by the Separations Research Program at the University of Texas, and by a National Science Foundation Graduate Research Fellowship. S.E.W. acknowledges very useful discussions with Dr. Bruce Weiner of Brookhaven Instruments concerning the design of the DLS scattering cell. D.R.M. and R.J.L. acknowledge the help of Cameron R. Youngstrom and Kyle W. Felling in the synthesis of the dansyl probe. We also thank Parag S. Shah and the Institute for Cell and Molecular Biology at the University of Texas for TEM assistance.

Supporting Information Available: UV−vis pyrene absorbances (PDF). This material is available free of charge via the Internet at http://pubs.acs.org.

JA025735D

(77) Mukerjee, P. In *Solution Chemistry of Surfactants*; Mittal, K. L., Ed.; Plenum Press: New York, 1979; Vol. 1.
(78) Miller, D. J.; Hawthorne, S. B. *Anal. Chem.* **1998**, *70*, 1618−1621.